

Lattice dynamics study of high-quality strontium bismuth tantalate single crystals

This article has been downloaded from IOPscience. Please scroll down to see the full text article.

2005 J. Phys.: Condens. Matter 17 7605

(<http://iopscience.iop.org/0953-8984/17/48/012>)

View [the table of contents for this issue](#), or go to the [journal homepage](#) for more

Download details:

IP Address: 129.252.86.83

The article was downloaded on 28/05/2010 at 06:53

Please note that [terms and conditions apply](#).

Lattice dynamics study of high-quality strontium bismuth tantalate single crystals

A Almeida¹, M R Chaves¹, H Amorin², M E V Costa² and A L Kholkin²

¹ Departamento de Física da Faculdade de Ciências, IFIMUP, Universidade do Porto, Rua do Campo Alegre, 687, 4169-007, Porto, Portugal

² Departamento de Engenharia Cerâmica e do Vidro, Universidade de Aveiro, CICECO, Campus Universitário de Santiago, 3810-193 Aveiro, Portugal

E-mail: amalmeid@fc.up.pt

Received 26 May 2005, in final form 10 October 2005

Published 11 November 2005

Online at stacks.iop.org/JPhysCM/17/7605

Abstract

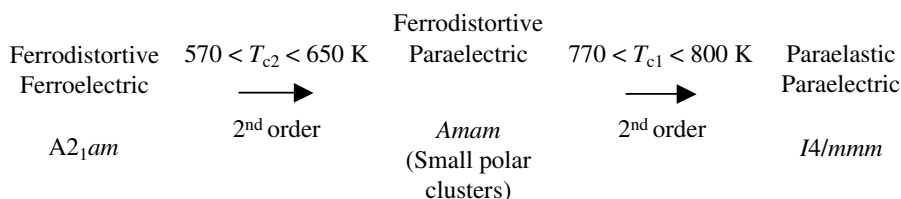
Raman scattering was investigated in high-quality SrBi₂Ta₂O₉ (SBT) single crystals prepared by the self-flux solution method. The Raman spectra in the range 6–1800 cm⁻¹ were monitored as a function of temperature both below and above the ferroelastic–ferroelectric phase transition at about 600 K. The behaviour of the soft ferroelectric mode and of its damping coefficient near the phase transition indicates a strong coupling with an acoustical phonon. The results provide clear evidence for a crossing over from a displacive to an order–disorder component and they are discussed in terms of a complex sequence of the phase transitions in SBT.

1. Introduction

Bi-layer structured ferroelectrics (BLSFs) have recently attracted a lot of attention due to a variety of useful ferroelectric, dielectric and piezoelectric properties accompanied by high Curie points. The advantage of these materials is also due to the absence of lead, that is going to be forbidden in Europe after 2006. The crystal structure of BLSFs consist of layers of pseudoperovskite blocks interleaved with bismuth oxide layers with a general formula (Bi₂O₂)²⁺(A_{m-1}B_mO_{3m+1})²⁻. Here *m* denotes the number of BO₆ octahedra, A can be mono-, di-, or trivalent metals (e.g., Na⁺, Sr²⁺, or Bi³⁺), and B represents small ions with high charge such as Ti⁴⁺, Nb⁵⁺, Ta⁵⁺, or W⁶⁺. One of the most studied representatives of the BLSF family is strontium bismuth tantalate (SrBi₂Ta₂O₉, SBT) because of its sufficiently high switching polarization, low coercive field, and, more importantly, the absence of ferroelectric fatigue, which has been the major obstacle for the commercialization of non-volatile ferroelectric memories (NVFRAMs) [1]. It was found [2] that the ferroelectric memory cells made with thin SBT films can withstand more than 10¹⁴ switching pulses, which is more than enough for the proper functioning of NVFRAM. Strontium bismuth tantalate is currently considered as a

major candidate for using in ferroelectric memories. It is also an important material due to its stable piezoelectric coefficients and high piezoelectric and dielectric anisotropy [3].

Ferroelectricity in SBT was discovered in the 1960s but has been very much studied in detail only in the last few years [4–14]. In SBT the $(\text{SrTa}_2\text{O}_7)^{2-}$ blocks composed of double TaO_6 octahedra with Sr at the A site are interleaved with $(\text{Bi}_2\text{O}_2)^{2+}$ layers. In this system, the $(\text{Bi}_2\text{O}_2)^{2+}$ layers are thought to control the electronic response (bandgaps, effective masses, etc) [10], while ferroelectric and dielectric anisotropy originates from the two-dimensional perovskite-like structure of pseudoperovskite units. For a long time, an intermediate phase between the high-symmetry tetragonal ($I4/mmm$) and the ferroelectric orthorhombic ($A2_1am$) phase has been suggested for some BLSFs, especially in cases with even m [12]. Recently, Onodera *et al* [8] have proposed the existence of an intermediate phase in SBT based on thermal behaviour and anomalous change of lattice parameters versus temperature. Powder neutron diffraction study in a polycrystalline sample of $\text{Sr}_{0.85}\text{Bi}_{2.1}\text{Ta}_2\text{O}_9$ showed that the room temperature ferroelectric phase (space group $A2_1am$) transforms at $T_{c2} \sim 648$ K, to a phase with the space group $Amam$ [13]. Macquart *et al* [14], by using the high-resolution powder neutron diffraction technique, have studied the structure of the different phases of SBT. This study revealed that both phase transitions are apparently continuous. The sequence of transitions presented in [14] is consistent with a group theoretical analysis. The transition from the $A2_1am$ to the $Amam$ structure involves not only loss of a displacive mode along the polar axis, but also the loss of a TaO_6 octahedral tilt mode around the c axis. Later, this intermediate phase was shown to be distortive and to occur between 570 K (distortive phase) and 770 K (ferroelastic–paraelastic). By using a polarized microscope, Kamba *et al* [6] disclosed the existence of ferroelastic domains in SBT single crystals up to 770 K. The gradual disappearance of domains on heating indicated that the transition from distortive to a para-phase ($770 \text{ K} < T_{c1} < 800 \text{ K}$) is near second order [6]. According to the ensemble of the results reported, the phase transition sequence currently assigned for SBT is the following:



It has been lately observed that the excess of Bi in SBT results in the increase of the lower transition temperature T_{c2} , and significantly increases the induced polarization, when Bi content is less than ~ 2.3 [15]. This behaviour undoubtedly testifies that Bi ions have an important contribution to the ferroelectric state [16]. The lowest-frequency phonon mode (around 28 cm^{-1}) observed in a number of reports [6, 17, 18] was shown to soften on heating but could not explain the dielectric constant anomaly and phase transition at T_{c2} [6]. The peculiarities of the phase transition in SBT were recently explained by coupling of this soft optical phonon mode with another hard vibration associated with the octahedral tilting at the Brillouin zone boundary (symmetry X_3^-) [19]. Therefore, the nature of the phase transition in SBT is much more complicated as compared to simple perovskites and requires further structural investigations.

The experimental studies of SBT were carried out mainly on ceramics and thin films and rarely on single crystals due to the lack of crystals of sufficient quality. Recently, Amorin *et al* [20] grew large SBT crystals where the anisotropy of dielectric and ferroelectric properties was reported for the first time [21]. In this work, we present a detailed Raman study of the external and internal modes as a function of temperature in these SBT crystals, with particular emphasis

on the soft mode behaviour. The results obtained in this paper provide clear evidence for a crossing over from a displacive to an order–disorder behaviour and for a low-frequency mode coupling which greatly contributes to the phase transition at T_{c2} . Moreover, it also corroborates the important role played by the $(\text{Bi}_2\text{O}_2)^{2+}$ units in the ferroelectric phase.

2. Experimental details

SBT single crystals were grown using a high-temperature modified self-flux solution method described elsewhere [20]. Plate-like SBT single crystals with rectangular shape and dimensions of approximately $5 \times 5 \times 0.2 \text{ mm}^3$ were used also for dielectric and P – E hysteresis measurements. X-ray diffraction analysis (XRD) showed a highly oriented single phase of SBT with the crystal edges oriented along the orthorhombic [110] direction ($\approx 45^\circ$ to both a and b axes) and the [001] direction (c axis) lying perpendicular to the major face. Lattice parameters were calculated from the XRD profile for the orthorhombic space group $A2_1am$: $a, b \cong 5.508(1) \text{ \AA}$ and $c \cong 25.01(1) \text{ \AA}$. These values are in a good agreement with the reported data [4–8]. The Raman spectra were obtained in the spectral range of 6 – 1800 cm^{-1} , using the polarized light of an Ar^+ laser, Coherent INNOVA 90 ($\lambda = 514.5 \text{ nm}$), in a back-scattering geometry. The unpolarized scattered light was analysed using a Jobin–Yvon T64000 spectrometer equipped with a CCD and a photon-counting detector. The spectral slit width was $\sim 1.5 \text{ cm}^{-1}$. The sample was placed in a furnace, with a temperature stability of 0.5 K in the temperature range 300 – 800 K . The spectra were registered at a constant temperature after a stabilization time of $\sim 15 \text{ min}$.

3. Results

Figures 1 and 2 show the depolarized Raman spectra taken from an SBT crystal at different temperatures between 299 and 613 K , detected by a CCD and by a photon counting detector, respectively. For further analysis, a sum of simple damped harmonic oscillators was used to fit the Raman spectra. In the frequency range 300 – 1000 cm^{-1} (figure 1) the bands associated with the internal modes of Bi_2O_2 and TaO_6 [16, 17] are indicated. The numerical analysis of the spectra between 150 and 320 cm^{-1} leads to the results depicted in figure 3. No significant anomalies were found in the wavenumber versus temperature [$\lambda^{-1}(T)$] for the different bands, but only small changes of the derivatives of $\lambda^{-1}(T)$ around 570 K were revealed. The integrated intensities of the bands labelled as III and IV, and associated with Ta^{5+} ion vibrations [7], show drastic changes with increasing temperature. While one grows larger with increasing temperature, the other one drastically decreases.

The spectra of external modes displayed in figure 2 disclose the soft optical phonon mode in a close agreement with previously reported results [6, 17]. In the same figure, the band centred at $\sim 77 \text{ cm}^{-1}$ is also shown, which is related to the vibrations of Bi in $(\text{Bi}_2\text{O}_2)^{2+}$ units, as already previously discussed [16, 17]. Figure 4 shows the resolved single-phonon features of the fit to the Raman data, in the low-frequency part (10 – 120 cm^{-1}), at three selected temperatures (493 , 553 and 583 K). Figures 5(a)–(d) present the wavenumber (λ^{-1}), the damping coefficient (γ), the squared frequency (ω^2) of the soft mode (I) versus temperature for these two low-frequency modes, and the temperature dependence of the real part of the electric susceptibility measured at the frequency of 50 kHz , along one direction in the plane ab . Below 570 K , $\lambda^{-1}(T)$ decreases slowly, with the temperature increase, followed by a sudden decrease around $T_{\text{cr}} = 570 \text{ K}$, while $\gamma(T)$ shows a divergence at T_{cr} . The expected function $\omega^2 = a(T - T_0)$ fits the experimental data, with $a = 4.5 \times 10^{22} (\text{Hz})^2 \text{ K}^{-1}$ and $T_0 = 891 \text{ K}$. Figures 5(a) and (b) also show respectively the temperature dependence of the wavenumber and of the damping coefficient for the band centred at $\sim 77 \text{ cm}^{-1}$ (II). The anomalous behaviour

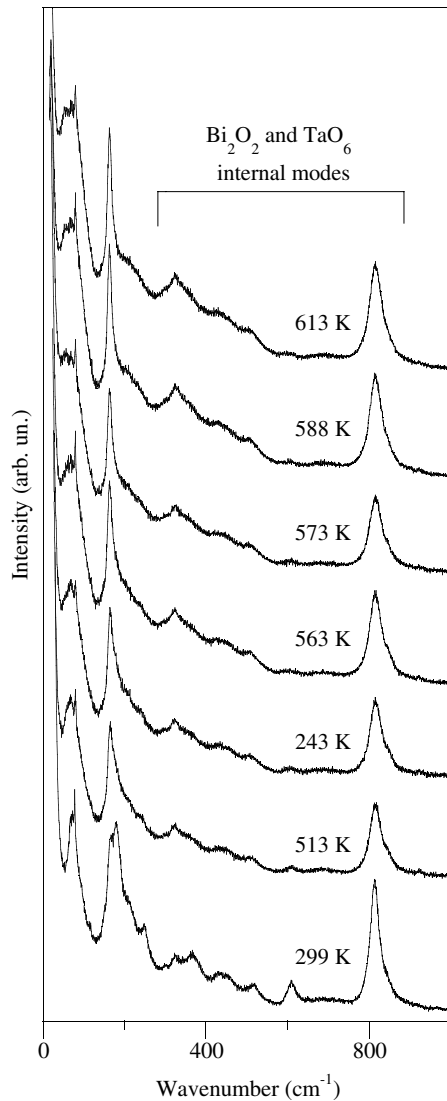


Figure 1. Unpolarized Raman spectra of SBT, for different fixed temperatures, obtained with a CCD detector.

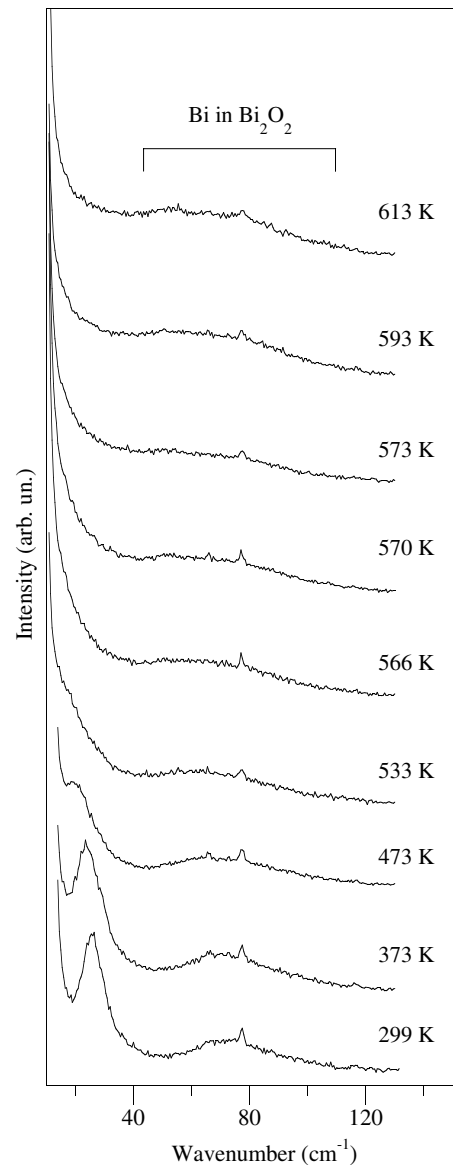


Figure 2. Unpolarized low-frequency Raman spectra of SBT for fixed different temperatures, obtained with a photon-counting detector.

of $\gamma(T)$ for the Bi–O mode corroborates the importance of the Bi–O interaction in the phase transition at T_{c2} .

4. Discussion

In addition to the soft mode, we have disclosed in SBT an overdamped mode above $T_{cr} = 570$ K centred at $\omega = 0$. The existence of a narrow peak centred at $\omega = 0$, referred to as central peak or central mode, is a dynamic feature, fairly common in structural phase transitions [22]. The

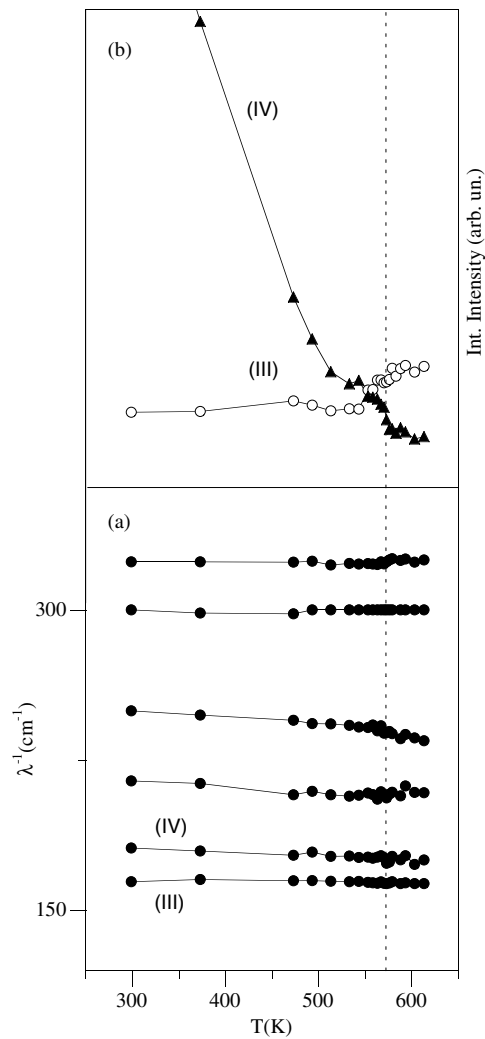


Figure 3. (a) Temperature dependence of the frequencies of the fitted Raman spectra shown in figure 1. The vertical dashed line marks the temperature T_{cr} . (b) Integrated intensities versus temperature of the bands labelled III and IV in figure 3(a).

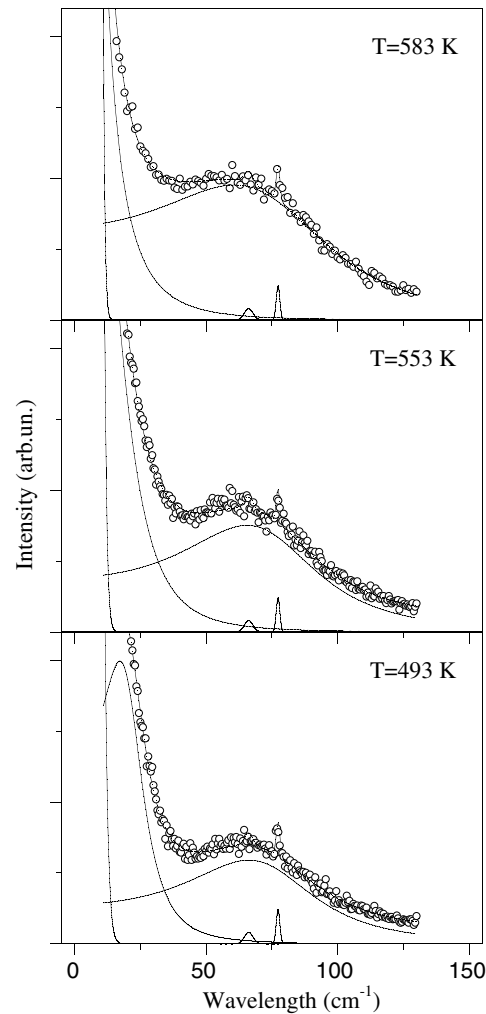


Figure 4. Fit to the Raman data, showing the resolved single-phonon features, in the low-frequency part ($10\text{--}120\text{ cm}^{-1}$), at three selected temperatures.

origin of the central peak can be related to a large variety of processes, such as microscopic clusters of a new structural phase, anharmonic interactions, direct coupling of light with phonon density fluctuations, and interaction of a soft mode with a relaxation mechanism [22]. The last process is particularly relevant when a soft mode of frequency ω_s interacts strongly with a relaxation mode with a relaxation time τ such as $1/\tau < \omega_s$, transferring in this way the mode strength to a central diffusive peak. In that picture, the central mode appears when the period of the soft mode oscillations becomes comparable to or less than the time required for a local temperature equilibrium to be established. Then the appearance of a central peak, and the arrest of the soft mode, can be accounted for.

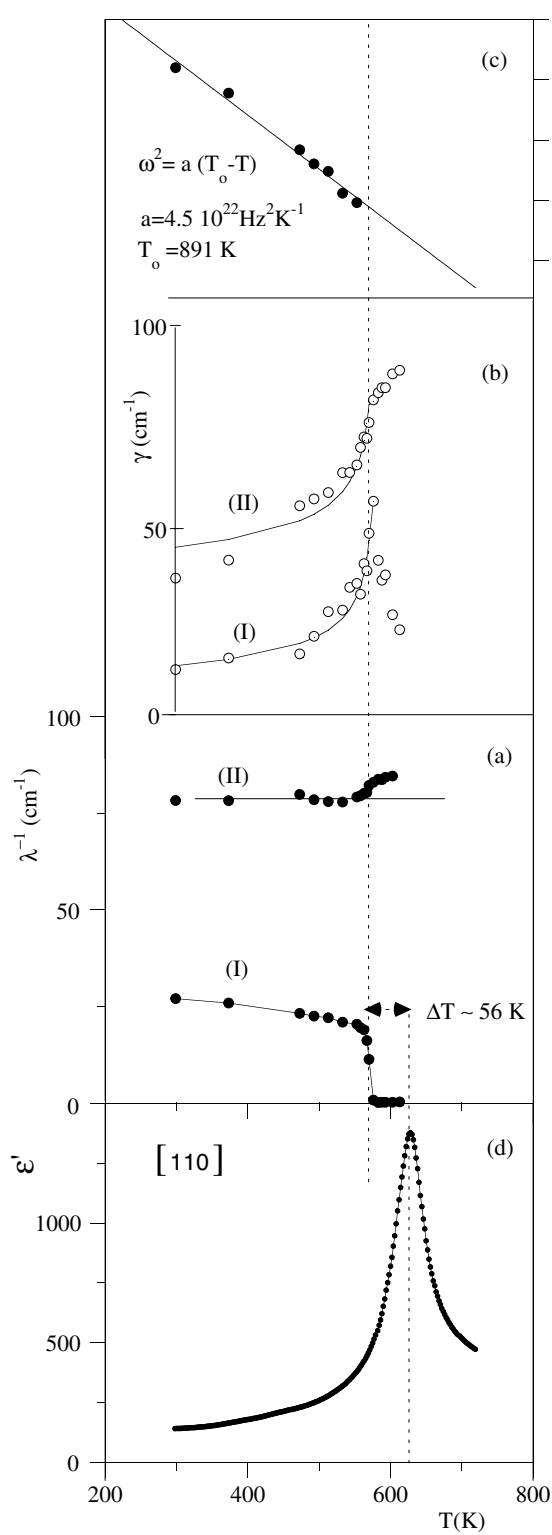


Figure 5. (a) Temperature dependence of the frequencies of the fitted Raman spectra shown in figure 2. (b) Temperature dependence of the damping coefficient of the bands I and II displayed in figure 5(a). Solid lines: fittings of equation (1) (see text) to the experimental data. (c) Squared frequency of band I (soft mode) versus temperature. The vertical dashed line marks the temperature T_{cr} . (d) Temperature dependence of the real part of the electric susceptibility, measured at a frequency of 50 kHz.

In SBT we observe an incomplete softening of the soft mode, with a large finite extrapolated value of ω^2 at T_{cr} , where the corresponding damping coefficient $\gamma(T)$ presents a maximum value. This large value of $\omega^2(T_{\text{cr}})$ is not due to a first-order character of the phase transition at T_{cr} . There is experimental evidence for a continuous phase transition at this temperature [14].

The temperature where the maximum of the low-frequency permittivity occurs is 56 K higher than T_{cr} , as can be seen in figure 5, in a crystal produced with the same technique as used to grow the crystal studied in Raman spectroscopy [21]. Taking into account the ensemble of these experimental results, it is plausible to assume that the incomplete softening in SBT is due to an interaction between the soft mode and another relaxation mechanism. The phase transition features disclose, in this way, a crossing over from a displacive to an order–disorder type, in the neighbourhood of T_{cr} . The condition written above ($1/\tau < \omega_s$) is verified; at T_{cr} we have ($1/50 < 1/25$), which is in agreement with the interpretation presented. When the displacements of the atoms attain a certain value, an order–disorder mechanism becomes important, giving also a relevant contribution to the permittivity, well above T_{cr} . Similarly, Zalar *et al* [23] have found evidence for the coexistence of displacive and order–disorder components in BaTiO_3 single crystals. The order–disorder dynamics is introduced by the relaxation motion of the Ti ion between several off-centre sites, while much faster displacive dynamics is due to the soft quasiharmonic oscillations around the equilibrium positions [23].

The soft mode has an E_u symmetry in the higher-temperature phase and is responsible for the spontaneous polarization. It can be roughly described as an antiphase displacement of the Bi atoms and of the perovskite blocks along the (1,1,0) direction of the tetragonal unit cell, plus a much smaller relative shift of the Sr and Ta cations with respect to the oxygen atoms in the perovskite blocks, while the O_3 ions in the Bi_2O_2 slabs remain fixed [19]. The hard mode at the frequency 75 cm^{-1} may be identified with the secondary mode of symmetry X^{2+} , considered by Perez-Mato *et al* [19]. It involves only the oxygen atoms within the Bi_2O_2 layers, and is essential for the final stabilization of the ferroelectric phase.

An anharmonic coupling of the soft mode E_u and the hard mode X^{2+} with an acoustic mode could explain the temperature dependence of the damping coefficient behaviour displayed in figure 5(b), below T_{cr} [24–26].

The empirical formula

$$\gamma = c + \frac{aT}{(T_{\text{cr}} - T)^{1/2}} + \frac{bT}{T_{\text{cr}} - T} \quad (1)$$

was successfully used to fit the temperature dependence of the damping coefficient when there is a coupling between an optical phonon and an acoustical phonon [24], and it was predicted theoretically, based on Landau theory [27]. This expression fits very well to the experimental collected data in SBT, as can be seen in figure 5. The values found for the different parameters are for band (I) $a = 0.22 \text{ K}^{-1/2} \text{ cm}^{-1}$, $b = -0.14 \text{ cm}^{-1}$, $c = 109 \text{ cm}^{-1}$ and $T_{\text{cr}} = 577 \text{ K}$, and for band (II) $a = 0.26 \text{ K}^{-1/2} \text{ cm}^{-1}$, $b = -0.19 \text{ cm}^{-1}$, $c = 139 \text{ cm}^{-1}$ and $T_{\text{cr}} = 577 \text{ K}$. The good fitting strongly corroborates the suggested coupling of optical and acoustic phonons in SBT.

Further experimental work is needed to identify properly the displacive and the order–disorder mechanisms in SBT and clarify the interesting issues raised by the analysis of the experimental results obtained in this material.

Acknowledgments

The authors are grateful to A Costa for his technical assistance. This work was supported by the project ‘Programa FEDER/POCTI (projecto no 2-155/94 da Fundação para a Ciência e a Tecnologia)’.

References

- [1] Paz de Araujo C A, Cucchiaro J D, McMillan L D, Scott M C and Scott J F 1995 *Nature* **374** 627
- [2] Auciello O, Scott J F and Ramesh R 1998 *Phys. Today* **51** 22
- [3] Damjanovic D 1998 *Curr. Opin. Solid State Mater. Sci.* **3** 469
- [4] Moret M P and Zallen R 1998 *Phys. Rev. B* **57** 5715
- [5] Yu T and Shen Z X 2003 *J. Appl. Phys.* **94** 618
- [6] Kamba S, Pokorny J, Porokhonsky V and Petzelt J 2002 *Appl. Phys. Lett.* **81** 1056
- [7] Zhu J S, Qin H X, Bao Z H and Wang Y N 2001 *Appl. Phys. Lett.* **79** 3827
- [8] Onodera A, Yoshio K and Yamashita H 2003 *J. Appl. Phys.* **42** 6218
- [9] Yoshio K, Matsubara I, Yamada A and Onodera A 2003 *J. Korean Phys. Soc.* **42** 1034
Noguchi Y, Miyayama M and Kudo T 2001 *Phys. Rev. B* **63** 214102(1)
- [10] Robertson J and Chen C W 1996 *Appl. Phys. Lett.* **69** 1704
- [11] Stachiotti M G, Rodriguez C O, Ambrosch-Draxl C and Christensen N E 2000 *Phys. Rev. B* **61** 14434
- [12] Nomura K, Takeda Y, Maeda M and Shibata N 2000 *Japan. J. Appl. Phys.* **39** 5247
- [13] Hervoche C H, Irvine J T S and Lightfoot P 2001 *Phys. Rev. B* **64** 100102(1)
- [14] Macquart R, Kennedy B J, Brett A H, Howard C J and Shimakawa Y 2002 *Intgr. Ferroelectr.* **44** 101
- [15] Noguchi Y, Miyayama M and Kudo T 2000 *J. Appl. Phys.* **88** 2147
- [16] Lee J-K, Park B and Hong K-S 2000 *J. Appl. Phys.* **88** 2825
- [17] Kojima S 1998 *J. Phys.: Condens. Matter* **10** L327
- [18] Kadlec F, Kamba S, Kuzel P, Kadlec C, Krouipa J and Petzelt J 2004 *J. Phys.: Condens. Matter* **16** 6763
- [19] Perez-Mato J M, Aroyo M, Garcia A, Blaha P, Schwartz K, Schweifer J and Parlinski K 2004 *Phys. Rev. B* **70** 214111
- [20] Amarin H, Costa M E V, Kholkin A L and Baptista J L 2004 *J. Eur. Ceram. Soc.* **24** 1535
- [21] Amarin H, Shvartsman V V, Kholkin A L and Costa M E V 2004 *Appl. Phys. Lett.* **85** 5667
- [22] Blinc R and Zeks B 1974 *Soft Modes in Ferroelectrics and Antiferroelectrics* (Amsterdam: North-Holland)
- [23] Zalar B, Laguta V V and Blinc R 2003 *Phys. Rev. B* **90** 037601(1)
- [24] Laulicht I, Bagno I and Schlesinger Y 1972 *J. Phys. Chem. Solids* **33** 319
- [25] Scott J F 1968 *Phys. Rev. Lett.* **21** 907
- [26] Burns G and Scott B A 1970 *Phys. Rev. Lett.* **25** 167
- [27] Levanyuk A P and Shchedrina N V 1974 *Sov. Phys.—Solid State* **16** 923